

1 Nonadiabatic dynamics studied by liquid-jet time-
2 resolved photoelectron spectroscopy

3 *Zachary N. Heim,[†] Daniel M. Neumark^{*, †, §}*

4 [†] Department of Chemistry, University of California, Berkeley, California 94720, United States

5 [§] Chemical Sciences Division, Lawrence Berkeley National Laboratory, Berkeley, California

6 94720, United States

7 CONSPECTUS

8 The development of the liquid microjet technique by Faubel and co-workers has enabled
9 the investigation of high vapor pressure liquids and solutions utilizing high-vacuum methods. One
10 such method is photoelectron spectroscopy (PES), which allows one to probe the electronic
11 properties of a sample through ionization in a state-specific manner. Liquid microjets consisting
12 of pure solvents and solute-solvent systems have been studied with great success utilizing PES and
13 its time-resolved corollary, TRPES. Here we discuss progress made over recent years in
14 understanding the solvation and excited state dynamics of the solvated electron and nucleic acid
15 constituents (NACs) using these methods, as well as the prospect for future applications of these
16 methods.

17 The solvated electron is of particular interest in liquid microjet experiments as it represents
18 the simplest solute system. Despite this simplicity, there were still many unresolved questions
19 about its binding energy and excited state relaxation dynamics that were ideal problems for liquid
20 microjet PES. In the work discussed in this Account, accurate binding energies were measured for
21 the solvated electron in multiple high vapor pressure solvents. The advantages of liquid jet PES
22 were further highlighted in the femtosecond excited state relaxation studies on the solvated
23 electron in water where a 75 ± 20 fs lifetime attributable to internal conversion from the excited
24 p-state to a hot ground state was measured, supporting a nonadiabatic relaxation mechanism.

25 Nucleic acid constituents represent a class of important solutes with several unresolved
26 questions that the liquid microjet PES method was uniquely suited to address. As TRPES is capable
27 of tracking dynamics with state-specificity, it is ideal for instances where there are multiple excited
28 states potentially involved in the dynamics. Time-resolved studies of NAC relaxation after
29 excitation using ultraviolet light identified relaxation lifetimes from multiple excited states. The
30 state-specific nature of the TRPES method allowed us to identify the lack of any signal attributable
31 to the $n\pi^*$ state in thymine derived NACs. The femtosecond time resolution of the technique also
32 aided in identifying differences between the excited state lifetimes of thymidine and thymidine

33 monophosphate. These have been interpreted, aided by molecular dynamics simulations, as an
34 influence of conformational differences leading to a longer excited state lifetime in thymidine
35 monophosphate.

36 Finally, advances in tabletop light sources extending into the extreme ultraviolet and soft
37 x-ray regimes to allow expansion of liquid jet TRPES to full valence and potentially core level
38 studies of solutes and pure liquids in liquid microjets is discussed. As most solutes have ground
39 state binding energies in the range of 10 eV, observation of both excited state decay and ground
40 state recovery using ultraviolet pump-ultraviolet probe TRPES has been intractable. With high-
41 harmonic generation light sources, it will be possible to not only observe full relaxation pathways
42 for valence level dynamics but to also track dynamics with element specificity by probing core
43 levels of the solute of interest.

44 KEY REFERENCES

- 45 • Erickson, B. A.; Heim, Z. N.; Pieri, E.; Liu, E.; Martinez, T. J.; Neumark, D. M. Relaxation
46 dynamics of hydrated thymine, thymidine, and thymidine monophosphate probed by liquid
47 jet time-resolved photoelectron spectroscopy. *J. Phys. Chem. A* **2019**, *123* (50), 10676-
48 10684.¹
- 49 • Williams, H. L.; Erickson, B. A.; Neumark, D. M. Time-resolved photoelectron
50 spectroscopy of adenosine and adenosine monophosphate photodeactivation dynamics in
51 water microjets. *J. Chem. Phys.* **2018**, *148*, 194303.²
- 52 • Elkins, M. H.; Williams, H. L.; Neumark, D. M. Dynamics of electron solvation in
53 methanol: Excited state relaxation and generation by charge-transfer-to-solvent. *J. Chem.*
54 *Phys.* **2015**, *142*, 234501.³
- 55 • Elkins, M. H.; Williams, H. L.; Shreve, A. T.; Neumark, D. M. Relaxation mechanism of
56 the hydrated electron. *Science* **2013**, *342*, 1496-1499.⁴

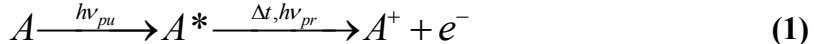
57

58 **1. Introduction**

59 The development of vacuum-compatible liquid water microjets, first reported in 1988,⁵ has
60 greatly expanded the range of chemical physics experiments that can be performed on water and
61 other volatile solvents. In particular, liquid jets enable one to apply very powerful tools based on
62 photoelectron spectroscopy to properties and dynamics of volatile solvents and the solutes
63 dissolved within. Photoelectron spectroscopy (PES) is a well-established technique in which a
64 sample is ionized, and the resulting electron kinetic energy distribution is measured. It is typically
65 used to determine electron binding energies and the electronic properties of gases and solids, but
66 its application to liquids were restricted to those with exceedingly low vapor pressures⁶ owing to
67 the high vacuum requirements of a photoelectron spectrometer. By applying PES to liquid
68 microjets in a vacuum, it has been possible to investigate the electronic properties of pure volatile
69 liquids⁷⁻¹⁰ and solutes.¹¹⁻¹² One photon PES measurements of binding energies have been used to
70 characterize the electronic structure of both pure liquids^{10, 13} and solutes,¹⁴⁻¹⁶ elucidating shifts in¹⁷

71 the binding energy in both solutes and individual solvent molecules due to interactions with
72 surrounding solvent. Experiments of this type represent an active frontier in modern physical
73 chemistry; in addition to providing a novel probe of structure and energetics within liquids, they
74 link gas phase studies of isolated molecules and clusters to chemical dynamics in the liquid phase.

75 A powerful variant of PES used in many areas of chemical dynamics is time-resolved
76 photoelectron spectroscopy (TRPES). TRPES is a pump-probe technique that is capable of
77 following the dynamical evolution of a excited state wavepacket.¹⁸ The overall experimental
78 scheme is as follows:



80 Typically, a femtosecond pump pulse photoexcites the system of interest, which then evolves in
81 time before being ionized by a femtosecond pulse that probes the evolution of the excited system.
82 The pump-induced dynamics are encoded in the resulting photoelectron kinetic energy
83 distribution, which is measured as a function of pump-probe delay. TRPES is particularly sensitive
84 to non-adiabatic transitions, since the various electronic states that participate in the dynamics tend
85 to have distinct electron binding energies. With pulses of sufficiently short duration and
86 appropriate wavelengths, TRPES can be used to track the complete relaxation process of a given
87 excited state from initial excitation through any intermediates that are populated en route to the
88 ground state. TRPES has been shown to have significant advantages including high sensitivity
89 stemming from exceptional intrinsic collection and detection efficiencies¹⁹ and allowing the direct
90 observation of the transient electronic states responsible for driving the ultrafast dynamics of
91 interest.¹² For these reasons, TRPES has for many years been an excellent tool for the study of
92 dynamics in both neutral and anionic gas phase molecules and clusters,¹⁸ as well as the
93 photophysics and photochemistry of metal and semiconductor surfaces.²⁰⁻²¹ With the advent of
94 liquid jet technology, it is now possible to apply TRPES to investigate the dynamics of
95 electronically excited solutes in bulk liquid,^{1, 4, 22-23} thereby adding a powerful new tool that
96 complements time-resolved techniques such as transient absorption²⁴⁻²⁶ and nonlinear
97 spectroscopies²⁷⁻²⁹ that have been used to investigate liquids for many years.

98 While liquid jet TRPES (LJ-TRPES) carries with it advantages intrinsic to the PES
99 technique, there are also limitations one must be cognizant of when interpreting LJ-TRPES results.
100 Probe depth has been a topic of considerable interest, as it relates directly to whether electrons
101 detected report on dynamics of solute molecules in bulk solution or in the vacuum-water interface.
102 Detailed simulations including effects of inelastic and elastic scattering show that even for a
103 photoelectron emitted with 35 eV kinetic energy, which is near the inelastic mean free path
104 minimum for electrons in liquid water,³⁰ approximately half the ejected photoelectrons originate
105 deeper than 3 water monolayers inside the liquid jets and could be considered bulk.³¹ Given these
106 results, it can be assumed most LJ-TRPES experiments can indeed probe bulk solute dynamics.
107 An added limitation of LJ-TRPES intrinsic to the PES technique is that of probe photon energy. A
108 TRPES experiment is only capable of observing dynamics involving electronic states in which the
109 probe photon energy is sufficient to photoionize/photodetach from a given region of a potential
110 surface.¹⁸ As such, insufficient probe photon energies can lead to a TRPES experiment being blind
111 to certain electronic states relevant to the complete relaxation dynamics of the system and can even

112 artificially shorten the observed lifetimes of electronic states with binding energies that are initially
113 within the observable range but fall outside of the observable range during the relaxation process.³²
114 This limitation has been a major motivating factor behind extending the probe photon energy range
115 of LJ-TRPES experiments into the XUV using high-harmonic generation.

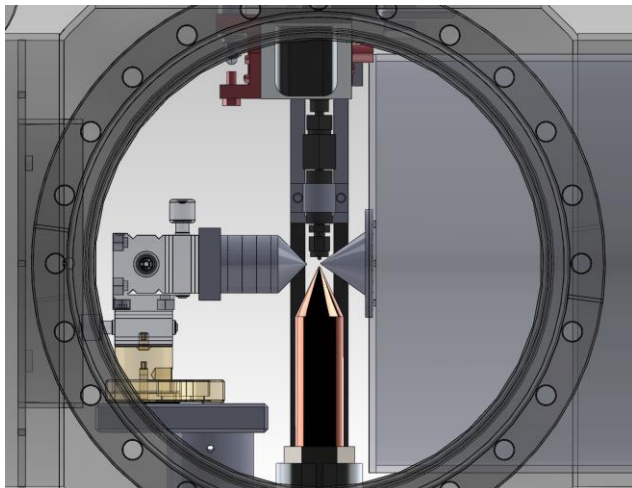
116 Particularly interesting applications of TRPES using liquid jets (LJ-TRPES) include the
117 investigation of benchmark condensed phase solutes such as the solvated electron and exploration
118 of the role that the solvent plays in the non-adiabatic relaxation dynamics of nucleic acid
119 constituents (NACs). The ground and excited states of the solvated electron have been well studied
120 in a variety of solvents using electron spin resonance, transient absorption, and photoelectron
121 spectroscopy in an effort to understand both its ground state structure and excited state relaxation
122 dynamics.³³ However, extraction of the p→s internal conversion (IC) lifetime from transient
123 absorption experiments is ambiguous,³⁴⁻³⁵ while LJ-TRPES yields a clear IC lifetime that is critical
124 in assessing the mechanism for electronic relaxation of the hydrated electron.⁴ The work on NACs
125 is motivated by experiments in the gas phase and in aqueous solution showing that excited state
126 lifetimes subsequent to ultraviolet excitation of nucleobases, nucleosides, nucleotides, and more
127 complex constituents are typically well under 1 ps.³⁶⁻³⁷ As a result, relaxation to the ground state
128 can occur more rapidly than excited state dissociation. These dynamics channel the electronic
129 energy deposited by the UV photon into vibrational excitation on the ground electronic state that
130 can be dissipated in the surrounding solvent, leading to the high photostability of DNA and its
131 constituents. Using a bottom-up approach, LJ-TRPES can in principle map out the complete set of
132 electronic states that participate in this mechanism and thus complement previous experimental
133 and theoretical work on NAC dynamics. To reach its full potential, however, the probe photon
134 energy used in LJ-TRPES experiments must be extended to be able to ionize the intermediate and
135 ground electronic states that play a role in the overall relaxation mechanism. This consideration
136 motivates the last section of this Account in which the beamline used to generate femtosecond
137 extreme ultraviolet (XUV) pulses is described.

138 2. Experimental Apparatus

139 The liquid microjet apparatus used for carrying out the photoelectron spectroscopy studies
140 discussed here has been modified since originally described^{3, 38} but at its core remains the same.
141 The design of the liquid microjet is based on the design developed by Wilson³⁹ and similar to the
142 type pioneered by Faubel.⁴⁰ In brief, the microjet is formed by forcing a solution through an
143 approximately 10 mm long segment of commercially available fused silica capillary with an inner
144 diameter ranging from 10 to 30 μm at pressures in the range of 40 to 120 atm. These microjet
145 diameters are necessary to satisfy the empirically determined conditions for collecting
146 photoelectrons while minimizing inelastic scattering in the surrounding vapor.¹⁰

147 The liquid microjet assembly, shown in Fig. 1, is affixed to a three-axis piezoelectric
148 actuator allowing it to be positioned 1 mm above the intersection of the detector and laser axes.
149 After passing through the interaction region, the jet can be frozen in a cryogenically cold vessel at
150 the bottom of the interaction region or captured in a heated copper catcher similar to those
151 implemented by Hummert et al.²³ and Riley et al.⁴¹ The catcher, which is affixed to the same
152 mounting apparatus as the jet, is kept approximately 1 cm below the jet and can be translated

153 independent of the jet for alignment purposes. The jet passes through a 500 μm aperture in the
154 catcher which is kept at 75°C and flows into a bottle kept in an ice bath and evacuated to a few
155 Torr to prevent vapor flow back into the interaction region. Catching the liquid as opposed to
156 freezing it has been shown to be advantageous as it mitigates the effects of electrokinetic charging
157 on the photoelectron spectrum⁴¹ in addition to lowering the measured chamber pressure by nearly
158 an order of magnitude.



159
160 **Figure 1.** Schematic diagram of the interaction region where the femtosecond pump and probe
161 pulses cross the liquid jet (from above) and subsequent photoelectrons are steered through a
162 skimmer (right) into the differentially pumped MB-TOF detector region by a strong permanent
163 magnet stack (left). Remaining sample is collected in the heated copper catcher (below)

164 Early work on liquid microjets in the Neumark group^{38, 42} utilized ultraviolet light
165 generated by frequency quadrupling or quintupling the output of a nanosecond Nd:YAG laser
166 which could then be used to excite and photoionize solutes of interest within the duration of a
167 single ~35 ns duration laser pulse. More recent explicitly time-resolved iterations of the
168 experiment^{1-4, 43} have utilized femtosecond pulses from a Ti:Sapphire oscillator/amplifier, the
169 output of which can then be frequency doubled, tripled, and quadrupled or directed into an optical
170 parametric amplifier to obtain ultraviolet pump and probe pulses with energies as high as 6.20 eV.
171 To achieve even higher probe photon energies, we have built a beamline employing high-harmonic
172 generation to selectively generate 21.7 eV photons (see Section 3.3). The femtosecond pulses are
173 delayed relative to one another and then cross the liquid microjet, emitting photoelectrons. The
174 photoelectrons are collected and energy-analyzed using a magnetic bottle time-of-flight
175 spectrometer and microchannel plate detector.⁴⁴

176 **3. Results and Discussion**

177 **3.1 Ultrafast Dynamics of Solvated Electrons**

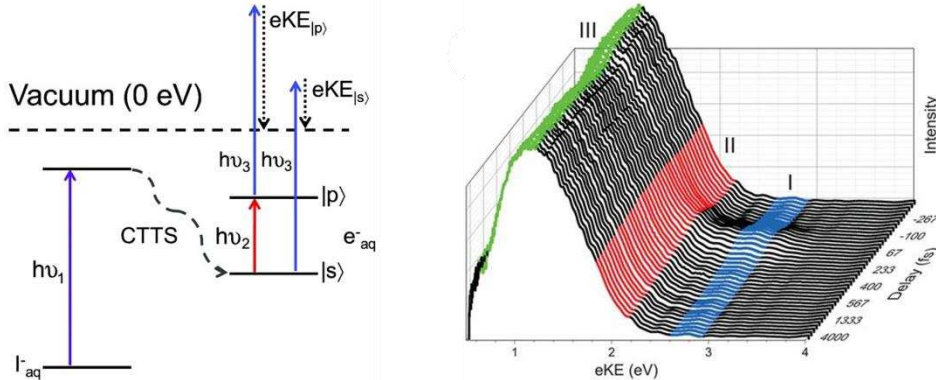
178 The solvated electron was the first system to be extensively studied by LJ-TRPES
179 experiments. This species is of fundamental interest in solution chemistry, as a reducing agent in
180 organic chemistry, a product in the radiolysis of water, and in the attachment to and subsequent

181 damage of DNA.⁴⁵ Its dynamics subsequent to photoexcitation have been investigated with an
182 impressive array of experimental³³ and theoretical⁴⁶ methods. From the perspective of gas phase
183 chemistry, water cluster anions (H_2O)_n⁻ have been studied using one-photon⁴⁷ and time-resolved
184 PES,⁴⁵ electronic spectroscopy,⁴⁸⁻⁴⁹ and vibrational spectroscopy,⁵⁰⁻⁵¹ with one goal being to
185 understand the relationship of these finite systems to the bulk hydrated electron. LJ-TRPES
186 experiments offer a unique and explicit link between the cluster and aqueous phase environments
187 of an excess electron in water. The primary focus of these experiments has been to determine the
188 vertical detachment energy of the hydrated electron and to probe its relaxation dynamics
189 subsequent to photoexcitation.

190 In solution, solvated electrons can be readily generated from a variety of simple solutes
191 such as iodide or ferrocyanide upon UV excitation of charge-transfer-to-solvent (CTTS)
192 transitions,⁵² adding to the simplicity of these studies. Initial LJ-PES investigations by Siefermann
193 et al.,⁵³ Tang et al.,⁵⁴ Lübcke et al.,⁵⁵ and Shreve et al.³⁸ yielded values ranging from 3.3-3.6 eV
194 for the binding energy of the bulk solvated electron, in good agreement with the values
195 extrapolated from measurements of internally solvated electrons in water cluster anion studies.⁴⁵
196⁴⁷ The work by Siefermann et al.⁵³ also included observation of a lower binding energy signal
197 assigned to surface bound electrons based on extrapolation of surface bound electron binding
198 energies in anion cluster experiments. While further experimental investigations have shown that
199 solute photodetachment can produce a transient population of interfacial electrons,⁵⁶ there is no
200 other experimental or theoretical evidence for stable surface-bound electrons in liquid jets.⁵⁷⁻⁵⁸
201 These initial LJ-PES measurements of the solvated electron binding energy remain in good
202 agreement with recent measurements yielding a value of 3.7 ± 0.1 eV that include corrections for
203 factors such as energy dependent scattering cross sections.³¹

204 Further studies on solvated electrons have demonstrated the utility of LJ-TRPES to
205 elucidate the time-resolved dynamics of these species. In aqueous solution, the solvated electron
206 can be excited to a manifold of p-states through excitation in the near-infrared and has been shown
207 through optical spectroscopy to relax back to the ground s-state with three time constants ranging
208 from 50 fs to 1 ps.^{35, 59} The interpretation of these time constants in terms of the overall relaxation
209 mechanism has been ambiguous. Two mechanisms have been invoked, the nonadiabatic and
210 adiabatic mechanisms.⁴⁶ These can in principle be distinguished by measuring the time constant
211 for p \rightarrow s internal conversion, which is on the order of 50 fs in the nonadiabatic model and 400 fs
212 in the adiabatic model. In size-selected water cluster anions, TRPES was used to measure this IC
213 lifetime; the extrapolation of these lifetimes to the bulk limit yielded value of \sim 60 fs, strongly
214 favoring the nonadiabatic model for relaxation.⁴⁵ However, given the uncertainty in how electrons
215 bind to finite water clusters and how the electron binding motif affects the excited state lifetime,⁶⁰
216 it seemed prudent to carry out TRPES in bulk water.

217



218

219 **Figure 2.** Left: Energy level diagram showing the states relevant to three pulse experiments in
 220 which solvated electrons are generated by CTTS excitation ($h\nu_1$) and the p-state relaxation
 221 dynamics are studied using an 800 nm pump ($h\nu_2$) and a 267 nm probe ($h\nu_3$). Right: LJ-TRPES
 222 spectra showing excited state relaxation of the solvated electron after 800 nm irradiation.
 223 Reproduced from Ref 4.

224 Using LJ-TRPES, experiments have been carried out as shown schematically in Figure 2.⁴
 225 Solvated electrons are generated from CTTS excitation of iodide at 240 nm after which an 800 nm
 226 pump pulse excites solvated electrons to the p-state and subsequent dynamics are tracked by a 267
 227 nm probe pulse and can be assigned unambiguously based on their respective binding energies.
 228 These experiments have also been used to observe the initial thermalization and recombination of
 229 electrons initially generated by the CTTS excitation prior to excitation by scanning the time delay
 230 between the CTTS pump and probe photons.³ In Figure 2, signal at a binding energy of 2.2 ± 0.2
 231 eV is assigned to the p-state and relaxes with a time constant of 75 ± 20 fs.⁴ This excited state
 232 population transfers to a region nearly 1 eV higher in binding energy, assigned to hot ground state
 233 signal, which then thermalizes with $\tau = 410 \pm 40$ fs. This study solidifies the nonadiabatic
 234 mechanistic picture of solvated electron relaxation as it directly observes the p-state relaxation,
 235 resolving differing interpretations of TA experiments. A subsequent investigation by Karashima et
 236 al.⁶¹ using time- and angle-resolved photoemission from a liquid microjet showed that the first
 237 component of the relaxation process, with a lifetime of 60 fs, was associated with anisotropic
 238 photoemission while the second component and ground state corresponded to isotropic
 239 photoemission. The evolving angular distribution reflects the change in orbital symmetry going
 240 from the excited p-state manifold to the ground s-state, supporting the assignment of the fast
 241 component in the excited state relaxation mechanism to a nonadiabatic transition from the excited
 242 state to a hot ground state. These results motivated similar LJ-TRPES experiments carried out on
 243 the solvated electron in D_2O ⁴³ and methanol,³ with resulting measurements of the internal
 244 conversion lifetime and solvent isotope effect also consistent with a nonadiabatic mechanism.

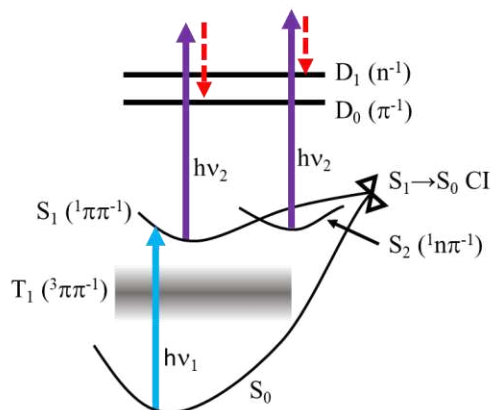
245

246 3.2 Ultrafast excited state dynamics in NACs

247 Nucleic acid constituents (NACs) have been studied widely³⁷ due both to their importance
 248 in biology as well as their complex photochemistry. NACs absorb light in the UV-C region with

249 large absorption bands near 270 nm and 200 nm attributed to $\pi\pi^*$ transitions.⁶² These wavelengths
 250 are typically destructive as the energy imparted on the molecule is on the order of typical bond
 251 dissociation energies.³⁶ Despite this, NACs have a remarkable photostability owing to ultrafast
 252 relaxation that efficiently funnels the excess electronic energy from the excited state into
 253 vibrational energy on the ground electronic surface, which can then be dissipated to the
 254 surrounding medium.^{37, 63} The underlying mechanism has been studied in solution using transient
 255 absorption (TA) and fluorescence upconversion (FU).^{36-37, 63} TRPES has been applied to this
 256 problem in both gas phase^{32, 64-66} and liquid jet^{1-2, 17, 67-68} experiments using UV pump and probe
 257 pulses. As was the case for hydrated electrons, a comparison of TRPES experiments in the gas
 258 phase and aqueous solution offers a unique opportunity to carry out complementary experiments
 259 of the same system in two very different environments.

260 The relaxation dynamics of NACs rely heavily on the relative position of the various
 261 possible excited states that could be involved, most notably the lowest energy $^1\pi\pi^*$, $^1n\pi^*$, and $^3\pi\pi^*$
 262 states, shown schematically in Figure 3 for aqueous thymine. In the gas phase, excitation in the
 263 270 nm band of isolated NACs populates the $^1\pi\pi^*$ state, which is energetically above both the $^1n\pi^*$
 264 and $^3\pi\pi^*$ states, allowing for population of these states as the molecule undergoes relaxation. In
 265 aqueous solution, this $^1\pi\pi^*$ state is stabilized relative to the nearby $^1n\pi^*$ state, as illustrated in Fig.
 266 3, putting it at comparable if not lower energy.¹⁷ The $^3\pi\pi^*$ state would also be stabilized in a
 267 comparable fashion. The relaxation pathways possible involving these states involve passage
 268 through a conical intersection (CI) from the $S_1(^1\pi\pi^*)$ state to the ground state, internal conversion
 269 to the $^1n\pi^*$ state, or intersystem crossing (ISC) to the $^3\pi\pi^*$ state shown in Figure 3.



270
 271 **Figure 3.** Schematic representation of the relevant electronic states involved of aqueous T, Thd,
 272 and TMP related to the relaxation dynamics subsequent to UV excitation.

273 In solution, TA experiments indicate notably different relaxation mechanisms for thymine
 274 and adenine derived NACs. In adenine, the relaxation was shown to involve only direct internal
 275 conversion through a CI from the S_1 excited state to the ground electronic state with no evidence
 276 of any contributions from intermediate excited states.⁶⁹ In thymine-derived NACs, TA
 277 experiments found a delay for ground state recovery that was attributed to intermediate excited
 278 states involved in the relaxation dynamics from the initially populated $^1\pi\pi^*$ state.⁷⁰⁻⁷¹ Early
 279 studies attributed this delay to a long-lived intermediate $^1n\pi^*$ state through which stepwise IC to

280 the ground state occurred.⁷⁰ This assignment has been called into question by more recent TA
281 studies, in which time-resolved UV/Vis and IR spectroscopy experiments of thymine and TMP
282 dissolved in either D₂O and CD₃CN were performed.⁷¹ In the gas phase, TRPES experiments
283 were carried out to observe the relaxation dynamics of isolated nucleobases.^{66, 72-73} These studies
284 show adenine and pyrimidine bases both have rapid transfer of population out of the initially
285 populated ¹ππ* state within <100 fs to an intermediate electronic state.^{66, 72} Later work was done
286 employing a higher energy probe capable of capturing a more complete picture of the relaxation
287 process, as earlier studies lacked sufficient probe energy to observe dynamics beyond ~1 ps. That
288 study showed that the ³ππ* state was populated from the ¹nπ* state in isolated thymine with a
289 rise time of approximately 3.5 ps.⁷³ These observations of rapid transfer of population to the ¹nπ*
290 state in gas phase TRPES experiments and the possible involvement of excited states other the
291 ¹ππ* state in solution serve as motivation to perform comparable TRPES experiments in aqueous
292 solution.

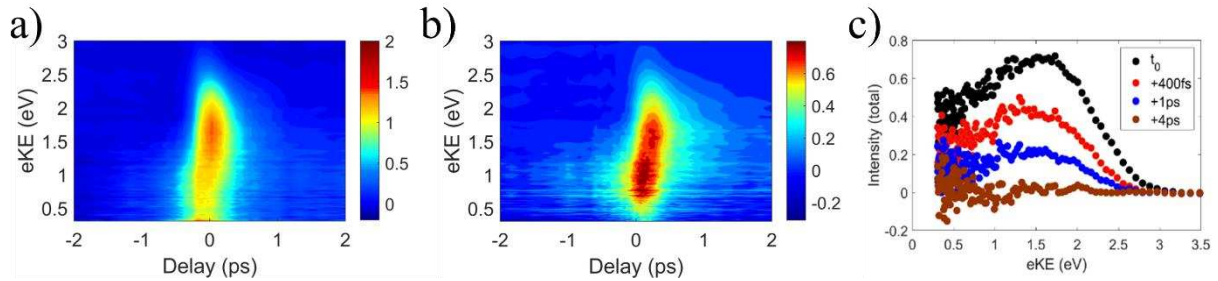
293 Initial experiments using liquid microjet TRPES to study NACs were performed by
294 Buchner et al, who observed femtosecond relaxation lifetimes of adenine, adenosine,⁶⁸ thymine,
295 thymidine,¹⁷ and guanosine⁶⁷ using a tunable UV (238 to 248 nm) and 267 nm pump-probe
296 scheme. For adenosine and adenine, they presented the first direct observation of the evolution of
297 excited NACs along a potential surface using femtosecond TRPES, providing valuable comparison
298 to theoretical studies⁷⁴ that had, up to that point, only the FU and TA experiments on solvated
299 NACs for comparison. The results obtained not only determined the lifetimes of the solvated
300 NACs, but also tracked the average kinetic energy of electrons from the excited state as a function
301 of time to infer dynamics of the population on the excited state surface itself. These studies were
302 then extended in our laboratory using a pump-probe scheme utilizing similar tunable UV pump
303 pulses and 200 nm rather than 267 nm probe pulses.^{1-2, 17, 68} This scheme extended the maximum
304 probe energy by 1 eV in an effort to observe as much of the dynamics as possible. We applied this
305 pump probe scheme to adenosine (Ado), thymine (T), and thymidine (Thd) in addition to
306 adenosine monophosphate (AMP) and thymidine monophosphate (TMP). Extending the LJ-
307 TRPES studies to include the nucleotides AMP and TMP was important to further the bottom-up
308 approach to understanding the dynamics in macromolecular DNA after radiation absorption. Key
309 results are as follows.

310 3.2.1 Relaxation from the S₁ ¹ππ*excited state

311 Figure 4 shows LJ-TRPES results for T and TMP at pump and probe energies of 4.74 and
312 6.20 eV, respectively. As discussed above, the relaxation dynamics from the S₁ ¹ππ* state in
313 aqueous T, Thd, and TMP have been hotly debated, with uncertainty surrounding the involvement
314 of the lowest lying ¹nπ*state in the relaxation from an initially prepared ¹ππ* state absorbing at
315 ~260 nm.³⁷ LJ-TRPES studies of T, Thd, and TMP find lifetimes for the S₁→S₀ relaxation in T and
316 Thd at 4.74 eV pump energy to be 360 fs and 390 fs respectively, in excellent agreement with
317 previous LJ-TRPES experiments and slightly shorter than but comparable to TA and FU
318 experiments. The corresponding lifetime in TMP is considerably longer, 870 fs, as can be seen by
319 comparing Figs. 4a and 4b. Moreover, no excited state signal is observed beyond 4 ps, as shown
320 in Figure 4c for T, even with the 6.2 eV probe energies employed. This observation adds further

321 evidence that the ${}^1n\pi^*$ state has no significant involvement in the relaxation dynamics of solvated
 322 T, Thd, and TMP. This state has been observed in the gas-phase as being long lived with a lifetime
 323 of approximately 10 ps and has a measured vertical ionization energy of 6.5 eV.⁷³ Given these
 324 values, one could expect any signal from the ${}^1n\pi^*$ state to appear with approximately 1 eV eKE
 325 given solvent stabilization of the resulting cationic state after photoionization. Lacking any
 326 persistent signal in this spectral region, the involvement of the ${}^1n\pi^*$ in the solution phase relaxation
 327 dynamics of thymine compounds is highly unlikely. Instead, it is possible the persistent signal seen
 328 in TA experiments is attributable to the ${}^3\pi\pi^*$ state, as predictions for the binding energy of this
 329 state lie anywhere from 0.6 eV above to 0.6 eV below the probe energy available in this experiment
 330 which would at best be near the lower detection limit of the detector used.

331



332

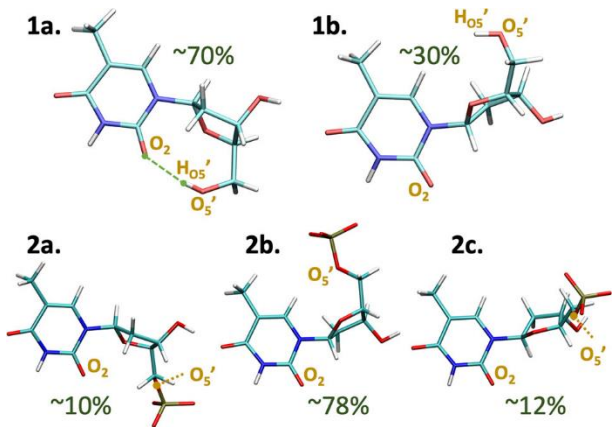
333 **Figure 4.** TRPE spectra of (a) thymine and (b) TMP showing 5.17 eV pump/6.20 eV probe data at
 334 positive delays and 6.20 eV pump/5.17 eV probe data at negative delays. (c) Static spectra at given
 335 delays for thymine show no identifiable signal past 4 ps. Reproduced from Ref. 1.

336 In LJ-TRPES experiments of aqueous Ado and AMP using the same TUV pump to excite
 337 to the $S_1 {}^1\pi\pi^*$ state, monoexponential excited state lifetimes on the order of 220 fs to 250 fs were
 338 found,² in general agreement with previous work.⁶⁸ Photoelectron spectra showed no delay
 339 dependent energy shifting of the excited state population, emphasizing the rapid timescales on
 340 which these dynamics occur. In addition, the $S_1 \rightarrow S_0$ lifetimes observed at the highest TUV pump
 341 energy of 4.97 eV was essentially identical to the lifetime observed when exciting at 4.69 eV, in
 342 contrast to previous work where the lifetime at 4.66 eV pump and 5.0 eV probe energies is
 343 approximately double the retrieved lifetime with those pump and probe energies switched.^{2,68} The
 344 difference in probe energy here is key; the previous study used a 4.66 eV probe while this work
 345 used a 6.2 eV probe, allowing observation of the full excited state wavepacket and retrieval of an
 346 accurate lifetime.

347 3.2.2 Differences in nucleotide relaxation lifetimes

348 Our experiments on TMP show that the lifetime of the $S_1 {}^1\pi\pi^*$ state of 870 fs at 4.74 eV
 349 pump energy is nearly double that of T (360 fs) and Thd (390 fs). While this trend had been
 350 observed previously in TA and FU experiments, no explanation for the substantial increase in
 351 lifetime for an excitation localized to the pyrimidine ring had been proposed. To this end, molecular
 352 dynamics simulations were performed, finding the dominant conformation of Thd present in
 353 solution to be the syn-conformer, shown in 1a of Figure 5.¹ However, in TMP the opposite
 354 conformation was more prevalent, putting the phosphate group near the C4-C5 side of the

355 pyrimidine ring. These conformational differences are important to consider as the dominant
 356 conical intersection predicted to be responsible for the rapid relaxation to the ground state in
 357 thymine-derived NACs is through distortion of the C4-C5 bond. The effects of these ground state
 358 conformational differences on the dynamics of the photoexcited species are currently under
 359 theoretical investigation.



361 **Figure 5.** Main conformers of Thd (1a and 1b) and TMP (2a, 2b, and 2c) determined by percentage
 362 occupation in a MM trajectory calculation. Reproduced from Ref. 1.

363 3.3 Future Prospects of Femtosecond XUV Probes

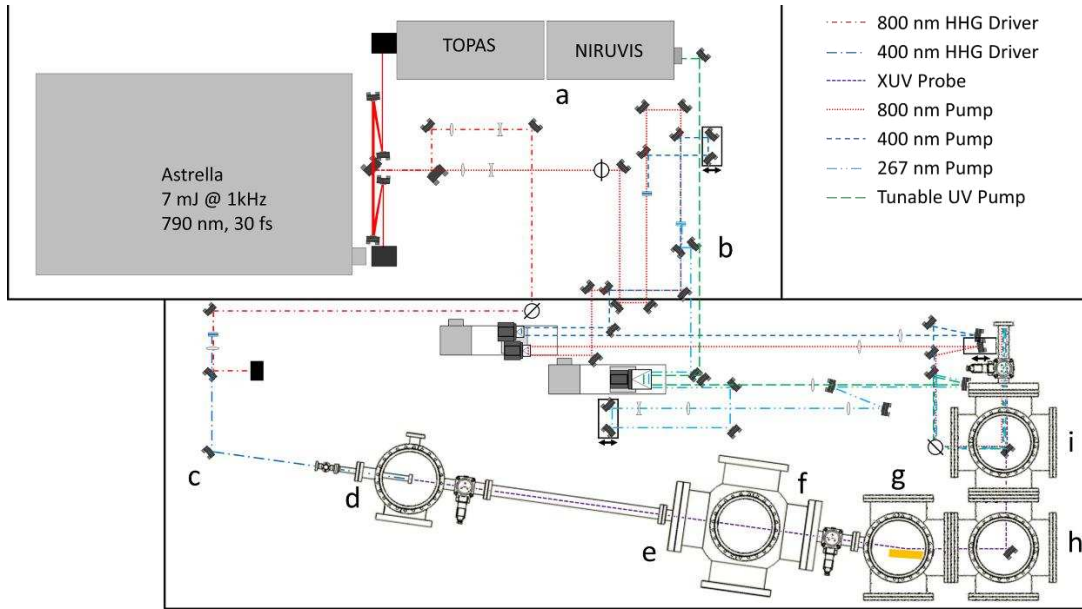
364 TRPES is capable, in principle, of tracking the complete relaxation pathway of a
 365 photoexcited system from the initially excited electronic state down to its ground state. The extent
 366 to which one can do this is determined by the probe photon energy and the type of system under
 367 study. In negative ion TRPES experiments, electron affinities are typically 5 eV or less. Hence,
 368 ground state negative ions can be photodetached by readily accessible UV femtosecond laser
 369 pulses that can be generated by standard nonlinear optical methods, such as frequency-tripling or
 370 quadrupling the 800 nm light produced by a Ti:Sapphire laser system to produce photons at 4.7 or
 371 6.2 eV, respectively. TRPES using femtosecond probe pulses at 7.9 eV produced by four-wave
 372 mixing has also recently been reported.⁷⁵ However, in TRPES experiments on neutral molecules
 373 in the gas phase and in solution, one must contend with ionization potentials that can be 10 eV or
 374 higher. Hence, the ability to generate femtosecond probe pulses in the extreme ultraviolet (XUV)
 375 region of the electromagnetic spectrum will significantly enhance the dynamical range of TRPES,
 376 as has been demonstrated in gas phase experiments using both table-top laser systems⁷⁶⁻⁷⁷ and free
 377 electron lasers.^{73, 78-79}

378 Advances in optical physics have brought about the high-harmonic generation (HHG)
 379 technique, in which high energy harmonics of a driving laser field can be generated by focusing
 380 the intense laser field into a diffuse gaseous medium.⁸⁰ These harmonics can be generated on a
 381 tabletop setup utilizing the same types of lasers typically used in TRPES experiments, so HHG is
 382 well suited for overcoming the aforementioned probe energy limitations, as was first demonstrated
 383 by Leone and co-workers on gas phase Br₂.⁷⁶ HHG sources for PES require relatively narrowband
 384 femtosecond pulses with energy resolution of the order of 10s to 100s of meV so as to minimize
 385 the width of photoelectron energy distributions from a given electronic state.⁸¹ To this effect, XUV

386 beamlines employing HHG yielding discrete harmonics and either multilayer mirrors or time-
387 compensating extreme ultraviolet (XUV) monochromators^{23, 82-84} have been built. These afford
388 temporal durations of XUV pulses on the order of 10s of femtoseconds while bandwidth in the
389 range of 200-500 meV is attainable. Various implementations of this approach have yielded
390 femtosecond high-harmonic sources with isolated harmonics ranging from 7 eV⁸⁴ to 100 eV.⁸⁵

391 LJ-TRPES using XUV probe pulses presents its own special challenges. Most notably, any
392 time-resolved dynamics resulting from photoexcitation and photoionization of solute molecules
393 competes with very strong signals from one-photon ionization of water, for which the vertical
394 ionization energy is 11.33 eV.⁸⁶ Nonetheless, several such experiments have already been
395 performed, ranging from fundamental processes in pure liquids to solute dynamics in systems such
396 as the solvated electron,¹² organic chromophores,^{23, 87} and organometallic complexes.⁸⁸ These
397 studies of increasingly complex molecules illustrate the trend towards larger systems that can be
398 effectively studied by the LJ-TRPES method given the advances in light sources and detector
399 technology.

400 The setup in our laboratory to carry out XUV TRPES on liquid jets is shown in Figure 6.
401 Here, 400 nm light is used to generate harmonics in a semi-infinite gas cell.⁸⁹ Driving harmonics
402 with 400 nm affords both a wide harmonic spacing of 6.2 eV and has the advantage of higher HHG
403 conversion efficiencies, as the efficiency scales with driving laser wavelength as approximately $\lambda^{-5} - \lambda^{-6}$,
404 though this also reduces the highest attainable photon energies.⁹⁰ Gas cell and focusing
405 parameters are optimized to maximize flux in the 7th harmonic of 400 nm (21.7 eV) and minimize
406 contributions from higher energy harmonics. The 7th harmonic is isolated using a multilayer mirror
407 developed by the Center for X-ray Optics at Lawrence Berkeley National Laboratory that is
408 designed to suppress the 5th and 9th harmonics while efficiently reflecting the 7th in conjunction
409 with an oxidized aluminum foil that both blocks the driving laser light and suppresses the 5th
410 harmonic at 15.5 eV. This design maximizes harmonic flux at the liquid jet by minimizing the
411 optics necessary to select and refocus a single harmonic, with only 3 optics in the harmonic
412 beamline reducing harmonic flux.



413

414 **Figure 6.** Optical layout used to generate pump and probe pulses in our XUV LJ-TRPES project.
 415 The layout consists of a) an OPA used to generate tunable UV light, b) a BBO-based third harmonic
 416 generation setup from which 267 nm, 400 nm, and 800 nm pump beams are derived, and c) a HHG
 417 beamline used to generate isolated 21.7 eV probe pulses consisting of d) a semi-infinite gas cell,
 418 e) a 200 nm thick Al filter, f) a beam analyzer for harmonic spectrum characterization, g) a toroidal
 419 mirror, h) a multilayer mirror that selectively reflects the 21.7 eV harmonic, and i) an annular
 420 mirror for pump-probe recombination.

421 Initial experiments will focus on using probe pulses at 21.7 eV to perform valence
 422 ionization of photoexcited neutral and ionic solutes. In the near future, we plan to extend our
 423 photon energy range into the soft x-ray regimes in order to take advantage of the elemental
 424 specificity offered by core-level photoelectron spectroscopy in liquids.¹⁴

425 **4. Concluding Remarks**

426 In this Account, the ultrafast dynamics of the solvated electron as well as thymine- and
 427 adenine-derived nucleic acid constituents as studied by liquid jet time-resolved photoelectron
 428 spectroscopy are summarized. These experiments, aimed at developing a greater understanding of
 429 the role solvent plays in relaxation dynamics, form the basis for insight into the initial dynamics
 430 relevant to DNA damage both indirectly by free electrons in solution and by direct absorption of
 431 ultraviolet light. The generation and relaxation of the solvated electron was investigated in H₂O,
 432 D₂O, and MeOH. In these studies, it was shown that an initially excited charge-transfer-to-solvent
 433 transition readily generates free electrons that persist for nanoseconds. When these electrons are
 434 photoexcited, p→s internal conversion occurs on a ~100 fs timescale in all three solvents. This
 435 timescale is consistent with the so-called nonadiabatic relaxation mechanism for solvated
 436 electrons. Additionally, experiments interrogating the relaxation dynamics of thymine- and
 437 adenine-derived NACs from the S₁ ¹ππ* state allowed measurement and comparison of lifetimes
 438 associated with these states across the different NACs. The thymine- and adenine-derived NACs

439 both show no evidence for intermediate states in relaxation from the $S_1\ ^1\pi\pi^*$ state. The thymine
440 NAC studies revealed a substantially longer lifetime for the S_1 excited state in TMP compared to
441 T and Thd; the source of this discrepancy was attributed to conformational changes from Thd to
442 TMP that could impact the excited state relaxation pathway. Finally, new tabletop XUV light
443 sources will enable carrying out LJ-TRPES experiments on a much wider variety of solutes and
444 afford access to more information in a given experiment through ionization of all valence states of
445 a solute.

446

447 AUTHOR INFORMATION

448 Corresponding Author

449 ***Daniel M. Neumark** – Email: dneumark@berkeley.edu

450 Author Contributions

451 The manuscript was written through contributions of all authors. All authors have given approval
452 to the final version of the manuscript. ‡These authors contributed equally. (match statement to
453 author names with a symbol)

454 BIOGRAPHICAL INFORMATION

455 **Zachary N. Heim** was born in 1994 in Sartell, Minnesota. He did his undergraduate studies at the
456 University of Wisconsin – Madison and graduated in 2017 with a B.S. in chemistry. Since then, he
457 has been working as a graduate student researcher in Daniel Neumark’s group at the University of
458 California at Berkeley.

459 <https://orcid.org/0000-0002-0240-7096>

460 **Daniel M. Neumark** was born in 1955 in Chicago, IL. He was an undergraduate at Harvard, then
461 went to graduate school at UC Berkeley. There, he worked in Yuan Lee’s research group and
462 received his Ph.D. in 1984. After spending two years at the University of Colorado, Boulder as a
463 post-doctoral fellow with Carl Lineberger, he joined the Berkeley Chemistry Department as an
464 Assistant Professor in 1986 and has been there ever since. His research interests encompass gas
465 phase studies of reaction dynamics via negative ion photodetachment, spectroscopy and scattering
466 experiments involving liquid microjets, and attosecond dynamics of atoms, molecules, and solids.

467 <https://orcid.org/0000-0002-3762-9473>

468 Notes

469 The authors declare no competing interests.

470 ACKNOWLEDGMENTS

471 This research is supported by the National Science Foundation Division of Chemistry under
472 Grant No. CHE-2154629.

473 **REFERENCES**

474 [1] Erickson, B. A.; Heim, Z. N.; Pieri, E.; Liu, E.; Martinez, T. J.; Neumark, D. M., Relaxation Dynamics
475 of Hydrated Thymine, Thymidine, and Thymidine Monophosphate Probed by Liquid Jet Time-Resolved
476 Photoelectron Spectroscopy. *The Journal of Physical Chemistry A* **2019**, *123*, 10676-10684.

477 [2] Williams, H. L.; Erickson, B. A.; Neumark, D. M., Time-resolved photoelectron spectroscopy of
478 adenosine and adenosine monophosphate photodeactivation dynamics in water microjets. *J. Chem. Phys.*
479 **2018**, *148*, 194303.

480 [3] Elkins, M. H.; Williams, H. L.; Neumark, D. M., Dynamics of electron solvation in methanol: Excited
481 state relaxation and generation by charge-transfer-to-solvent. *The Journal of Chemical Physics* **2015**, *142*,
482 234501.

483 [4] Elkins, M. H.; Williams, H. L.; Shreve, A. T.; Neumark, D. M., Relaxation Mechanism of the Hydrated
484 Electron. *Science* **2013**, *342*, 1496-1499.

485 [5] Faubel, M.; Schlemmer, S.; Toennies, J. P., A molecular beam study of the evaporation of water
486 from a liquid jet. *Z. Phys. D: At., Mol. Clusters* **1988**, *10*, 269-277.

487 [6] Siegbahn, H., Electron spectroscopy for chemical analysis of liquids and solutions. *The Journal of
488 Physical Chemistry* **1985**, *89*, 897-909.

489 [7] Yamamoto, Y.-i.; Ishiyama, T.; Morita, A.; Suzuki, T., Exploration of Gas–Liquid Interfaces for Liquid
490 Water and Methanol Using Extreme Ultraviolet Laser Photoemission Spectroscopy. *The Journal of Physical
491 Chemistry B* **2021**, *125*, 10514-10526.

492 [8] Longetti, L.; Randulová, M.; Ojeda, J.; Mewes, L.; Miseikis, L.; Grilj, J.; Sanchez-Gonzalez, A.;
493 Witting, T.; Siegel, T.; Diveki, Z.; van Mourik, F.; Chapman, R.; Cacho, C.; Yap, S.; Tisch, J. W. G.; Springate,
494 E.; Marangos, J. P.; Slavíček, P.; Arrell, C. A.; Chergui, M., Photoemission from non-polar aromatic molecules
495 in the gas and liquid phase. *Physical Chemistry Chemical Physics* **2020**, *22*, 3965-3974.

496 [9] Nishitani, J.; West, C. W.; Suzuki, T., Angle-resolved photoemission spectroscopy of liquid water at
497 29.5 eV. *Structural Dynamics* **2017**, *4*, 044014.

498 [10] Faubel, M.; Steiner, B.; Toennies, J. P., Photoelectron Spectroscopy of Liquid Water, some Alcohols,
499 and Pure Nonane in Free Micro Jets. *J. Chem. Phys.* **1997**, *106*, 9013-9031.

500 [11] Buttersack, T.; Mason, P. E.; McMullen, R. S.; Schewe, H. C.; Martinek, T.; Brezina, K.; Crhan, M.;
501 Gomez, A.; Hein, D.; Wartner, G.; Seidel, R.; Ali, H.; Thürmer, S.; Marsalek, O.; Winter, B.; Bradforth, S. E.;
502 Jungwirth, P., Photoelectron spectra of alkali metal-ammonia microjets: From blue electrolyte to bronze
503 metal. *Science* **2020**, *368*, 1086-1091.

504 [12] Nishitani, J.; Yamamoto, Y.-i.; West, C. W.; Karashima, S.; Suzuki, T., Binding energy of solvated
505 electrons and retrieval of true UV photoelectron spectra of liquids. *Science Advances* **2019**, *5*, eaaw6896.

506 [13] Schewe, H. C.; Brezina, K.; Kostal, V.; Mason, P. E.; Buttersack, T.; Stemer, D. M.; Seidel, R.; Quevedo,
507 W.; Trinter, F.; Winter, B.; Jungwirth, P., Photoelectron Spectroscopy of Benzene in the Liquid Phase and
508 Dissolved in Liquid Ammonia. *The Journal of Physical Chemistry B* **2022**, *126*, 229-238.

509 [14] Winter, B.; Weber, R.; Hertel, I. V.; Faubel, M.; Jungwirth, P.; Brown, E. C.; Bradforth, S. E., Electron
510 binding energies of aqueous alkali and halide ions: EUV photoelectron spectroscopy of liquid solutions and
511 combined ab initio and molecular dynamics calculations. *Journal of the American Chemical Society* **2005**,
512 *127*, 7203-7214.

513 [15] Winter, B.; Faubel, M., Photoemission from Liquid Aqueous Solutions. *Chemical Reviews* **2006**,
514 *106*, 1176-1211.

515 [16] Seidel, R.; Thürmer, S.; Winter, B., Photoelectron Spectroscopy Meets Aqueous Solution: Studies
516 from a Vacuum Liquid Microjet. *The Journal of Physical Chemistry Letters* **2011**, *2*, 633-641.

517 [17] Buchner, F.; Nakayama, A.; Yamazaki, S.; Ritze, H. H.; Lübcke, A., Excited-State Relaxation of
518 Hydrated Thymine and Thymidine Measured by Liquid-Jet Photoelectron Spectroscopy: Experiment and
519 Simulation. *J. Am. Chem. Soc.* **2015**, *137*, 2931-2938.

520 [18] Stolow, A.; Bragg, A. E.; Neumark, D. M., Femtosecond Time-Resolved Photoelectron
521 Spectroscopy. *Chem. Rev.* **2004**, *104*, 1719-1758.

522 [19] Buchner, F.; Schultz, T.; Lübcke, A., Solvated electrons at the water-air interface: Surface versus
523 bulk signal in low kinetic energy photoelectron spectroscopy. *Phys. Chem. Chem. Phys.* **2012**, *14*,
524 58375842.

525 [20] Siefermann, K. R.; Pemmaraju, C. D.; Neppl, S.; Shavorskiy, A.; Cordones, A. A.; Vura-Weis, J.;
526 Slaughter, D. S.; Sturm, F. P.; Weise, F.; Bluhm, H.; Strader, M. L.; Cho, H.; Lin, M.-F.; Bacellar, C.; Khurmi, C.;
527 Guo, J.; Coslovich, G.; Robinson, J. S.; Kaindl, R. A.; Schoenlein, R. W.; Belkacem, A.; Neumark, D. M.; Leone,
528 S. R.; Nordlund, D.; Ogasawara, H.; Krupin, O.; Turner, J. J.; Schlotter, W. F.; Holmes, M. R.; Messerschmidt,
529 M.; Minitti, M. P.; Gul, S.; Zhang, J. Z.; Huse, N.; Prendergast, D.; Gessner, O., Atomic-Scale Perspective of
530 Ultrafast Charge Transfer at a Dye–Semiconductor Interface. *The Journal of Physical Chemistry Letters*
531 **2014**, *5*, 2753-2759.

532 [21] Neppl, S.; Gessner, O., Time-resolved X-ray photoelectron spectroscopy techniques for the study
533 of interfacial charge dynamics. *Journal of Electron Spectroscopy and Related Phenomena* **2015**, *200*, 64-
534 77.

535 [22] Buchner, F.; Lübcke, A.; Heine, N.; Schultz, T., Time-resolved photoelectron spectroscopy of liquids.
536 *Review of Scientific Instruments* **2010**, *81*, 113107.

537 [23] Hummert, J.; Reitsma, G.; Mayer, N.; Ikonnikov, E.; Eckstein, M.; Kornilov, O., Femtosecond
538 Extreme Ultraviolet Photoelectron Spectroscopy of Organic Molecules in Aqueous Solution. *The Journal of
539 Physical Chemistry Letters* **2018**, *9*, 6649-6655.

540 [24] Kumpulainen, T.; Lang, B.; Rosspeintner, A.; Vauthey, E., Ultrafast Elementary Photochemical
541 Processes of Organic Molecules in Liquid Solution. *Chemical Reviews* **2017**, *117*, 10826-10939.

542 [25] Berera, R.; van Grondelle, R.; Kennis, J. T. M., Ultrafast transient absorption spectroscopy:
543 principles and application to photosynthetic systems. *Photosynthesis Research* **2009**, *101*, 105-118.

544 [26] Kovalenko, S. A.; Schanz, R.; Hennig, H.; Ernsting, N. P., Cooling dynamics of an optically excited
545 molecular probe in solution from femtosecond broadband transient absorption spectroscopy. *The Journal
546 of Chemical Physics* **2001**, *115*, 3256-3273.

547 [27] Auböck, G.; Consani, C.; van Mourik, F.; Chergui, M., Ultrabroadband femtosecond two-
548 dimensional ultraviolet transient absorption. *Optics Letters* **2012**, *37*, 2337-2339.

549 [28] Khalil, M.; Demirdöven, N.; Tokmakoff, A., Coherent 2D IR Spectroscopy: Molecular Structure and
550 Dynamics in Solution. *The Journal of Physical Chemistry A* **2003**, *107*, 5258-5279.

551 [29] Hybl, J. D.; Ferro, A. A.; Jonas, D. M., Two-dimensional Fourier transform electronic spectroscopy.
552 *The Journal of Chemical Physics* **2001**, *115*, 6606-6622.

553 [30] Seidel, R.; Winter, B.; Bradforth, S. E., Valence Electronic Structure of Aqueous Solutions: Insights
554 from Photoelectron Spectroscopy. *Annual Review of Physical Chemistry* **2016**, *67*, 283-305.

555 [31] Luckhaus, D.; Yamamoto, Y.-i.; Suzuki, T.; Signorell, R., Genuine binding energy of the hydrated
556 electron. *Science Advances* **2017**, *3*, e1603224.

557 [32] Hudock, H. R.; Levine, B. G.; Thompson, A. L.; Satzger, H.; Townsend, D.; Gador, N.; Ullrich, S.;
558 Stolow, A.; Martínez, T. J., Ab Initio Molecular Dynamics and Time-Resolved Photoelectron Spectroscopy
559 of Electronically Excited Uracil and Thymine. *The Journal of Physical Chemistry A* **2007**, *111*, 8500-8508.

560 [33] Herbert, J. M.; Coons, M. P., The Hydrated Electron. *Annual Review of Physical Chemistry* **2017**, *68*,
561 447-472.

562 [34] Yokoyama, K.; Silva, C.; Son, D. H.; Walhout, P. K.; Barbara, P. F., Detailed Investigation of the
563 Femtosecond Pump-Probe Spectroscopy of the Hydrated Electron. *The Journal of Physical Chemistry A*
564 **1998**, *102*, 6957-6966.

565 [35] Pshenichnikov, M. S.; Baltuška, A.; Wiersma, D. A., Hydrated-electron population dynamics.
566 *Chemical Physics Letters* **2004**, *389*, 171-175.

567 [36] Schreier, W. J.; Gilch, P.; Zinth, W., Early Events of DNA Photodamage. *Annual Review of Physical*
568 *Chemistry* **2015**, *66*, 497-519.

569 [37] Middleton, C. T.; Harpe, K. d. L.; Su, C.; Law, Y. K.; Crespo-Hernández, C. E.; Kohler, B., DNA Excited-
570 State Dynamics: From Single Bases to the Double Helix. *Annual Review of Physical Chemistry* **2009**, *60*,
571 217-239.

572 [38] Shreve, A. T.; Yen, T. A.; Neumark, D. M., Photoelectron spectroscopy of hydrated electrons.
573 *Chemical Physics Letters* **2010**, *493*, 216-219.

574 [39] Wilson, K. R.; Rude, B. S.; Smith, J.; Cappa, C.; Co, D. T.; Schaller, R. D.; Larsson, M.; Catalano, T.;
575 Saykally, R. J.; A., B.; M., D.; S., P. P.; H., W. A.; J., A.-N.; J., B., Investigation of volatile liquid surfaces by
576 synchrotron x-ray spectroscopy of liquid microjets. *Review of Scientific Instruments* **2004**, *75*, 725-736.

577 [40] Faubel, M.; Steiner, B.; Toennies, J. P., Measurement of He I photoelectron spectra of liquid water,
578 formamide and ethylene glycol in fast-flowing microjets. *J. Electron Spectrosc. Relat. Phenom.* **1998**, *95*,
579 159-169.

580 [41] Riley, J. W.; Wang, B.; Parkes, M. A.; Fielding, H. H.; R., A. M. N., Design and characterization of a
581 recirculating liquid-microjet photoelectron spectrometer for multiphoton ultraviolet photoelectron
582 spectroscopy. *Review of Scientific Instruments* **2019**, *90*, 083104.

583 [42] Shreve, A. T.; Elkins, M. H.; Neumark, D. M., Photoelectron spectroscopy of solvated electrons in
584 alcohol and acetonitrile microjets. *Chemical Science* **2013**, *4*, 1633-1639.

585 [43] Elkins, M. H.; Williams, H. L.; Neumark, D. M., Isotope effect on hydrated electron relaxation
586 dynamics studied with time-resolved liquid jet photoelectron spectroscopy. *The Journal of Chemical*
587 *Physics* **2016**, *144*, 184503.

588 [44] Kruit, P.; Read, F. H., Magnetic Field Paralleliser for 2PI Electron-Spectrometer and Electron-Image
589 Magnifier. *J. Phys. E: Sci. Instrum.* **1983**, *16*, 313-324.

590 [45] Young, R. M.; Neumark, D. M., Dynamics of Solvated Electrons in Clusters. *Chemical Reviews* **2012**,
591 *112*, 5553-5577.

592 [46] Turi, L.; Rossky, P. J., Theoretical Studies of Spectroscopy and Dynamics of Hydrated Electrons.
593 *Chem. Rev.* **2012**, *112*, 5641-5674.

594 [47] Coe, J. V.; Lee, G. H.; Eaton, J. G.; Arnold, S. T.; Sarkas, H. W.; Bowen, K. H.; Ludewigt, C.; Haberland,
595 H.; Worsnop, D. R., Photoelectron spectroscopy of hydrated electron cluster anions, (H₂O)_n=2-69. *The*
596 *Journal of Chemical Physics* **1990**, *92*, 3980-3982.

597 [48] Ayotte, P.; Johnson, M. A., Electronic absorption spectra of size-selected hydrated electron
598 clusters: (H₂O)_n-, n=6-50. *The Journal of Chemical Physics* **1997**, *106*, 811-814.

599 [49] Herburger, A.; Barwa, E.; Ončák, M.; Heller, J.; van der Linde, C.; Neumark, D. M.; Beyer, M. K.,
600 Probing the Structural Evolution of the Hydrated Electron in Water Cluster Anions (H₂O)_n-, n ≤ 200, by
601 Electronic Absorption Spectroscopy. *Journal of the American Chemical Society* **2019**, *141*, 18000-18003.

602 [50] Hammer, N. I.; Shin, J.-W.; Headrick, J. M.; Diken, E. G.; Roscioli, J. R.; Weddle, G. H.; Johnson, M.
603 A., How Do Small Water Clusters Bind an Excess Electron? *Science* **2004**, *306*, 675-679.

604 [51] Asmis, K. R.; Santambrogio, G.; Zhou, J.; Garand, E.; Headrick, J.; Goebbert, D.; Johnson, M. A.;
605 Neumark, D. M., Vibrational spectroscopy of hydrated electron clusters(H₂O)15-50- via infrared multiple
606 photon dissociation. *The Journal of Chemical Physics* **2007**, *126*, 191105.

607 [52] Hart, E. J.; Boag, J. W., Absorption Spectrum of the Hydrated Electron in Water and in Aqueous
608 Solutions. *J. Am. Chem. Soc.* **1962**, *84*, 4090-4095.

609 [53] Siefermann, K. R.; Liu, Y.; Lugovoy, E.; Link, O.; Faubel, M.; Buck, U.; Winter, B.; Abel, B., Binding
610 energies, lifetimes and implications of bulk and interface solvated electrons in water. *Nature Chemistry*
611 **2010**, *2*, 274-279.

612 [54] Tang, Y.; Suzuki, Y.-i.; Shen, H.; Sekiguchi, K.; Kurahashi, N.; Nishizawa, K.; Zuo, P.; Suzuki, T., Time-
613 resolved photoelectron spectroscopy of bulk liquids at ultra-low kinetic energy. *Chemical Physics Letters*
614 **2010**, *494*, 111-116.

615 [55] Lübcke, A.; Buchner, F.; Heine, N.; Hertel, I. V.; Schultz, T., Time-resolved photoelectron
616 spectroscopy of solvated electrons in aqueous NaI solution. *Phys. Chem. Chem. Phys.* **2010**, *12*, 14629.

617 [56] Jordan, C. J. C.; Lowe, E. A.; Verlet, J. R. R., Photooxidation of the Phenolate Anion is Accelerated
618 at the Water/Air Interface. *Journal of the American Chemical Society* **2022**, *144*, 14012-14015.

619 [57] Uhlig, F.; Marsalek, O.; Jungwirth, P., Electron at the Surface of Water: Dehydrated or Not? *Journal*
620 *of Physical Chemistry Letters* **2013**, *4*, 338-343.

621 [58] Coons, M. P.; You, Z.-Q.; Herbert, J. M., The Hydrated Electron at the Surface of Neat Liquid Water
622 Appears To Be Indistinguishable from the Bulk Species. *Journal of the American Chemical Society* **2016**,
623 *138*, 10879-10886.

624 [59] Assel, M.; Laenen, R.; Laubereau, A., Femtosecond solvation dynamics of solvated electrons in
625 neat water. *Chemical Physics Letters* **2000**, *317*, 13-22.

626 [60] Borgis, D.; Rossky, P. J.; Turi, L., Electronic Excited State Lifetimes of Anionic Water Clusters:
627 Dependence on Charge Solvation Motif. *Journal of Physical Chemistry Letters* **2017**, *8*, 2304-2309.

628 [61] Karashima, S.; Yamamoto, Y.-i.; Suzuki, T., Resolving Nonadiabatic Dynamics of Hydrated Electrons
629 Using Ultrafast Photoemission Anisotropy. *Physical Review Letters* **2016**, *116*, 137601.

630 [62] Voet, D.; Gratzer, W. B.; Cox, R. A.; Doty, P., Absorption spectra of nucleotides, polynucleotides,
631 and nucleic acids in the far ultraviolet. *Biopolymers* **1963**, *1*, 193-208.

632 [63] Pecourt, J.-M. L.; Peon, J.; Kohler, B., DNA Excited-State Dynamics: Ultrafast Internal Conversion
633 and Vibrational Cooling in a Series of Nucleosides. *Journal of the American Chemical Society* **2001**, *123*,
634 10370-10378.

635 [64] Evans, N. L.; Ullrich, S., Wavelength Dependence of Electronic Relaxation in Isolated Adenine Using
636 UV Femtosecond Time-Resolved Photoelectron Spectroscopy. *The Journal of Physical Chemistry A* **2010**,
637 *114*, 11225-11230.

638 [65] Satzger, H.; Townsend, D.; Zgierski, M. Z.; Patchkovskii, S.; Ullrich, S.; Stolow, A., Primary processes
639 underlying the photostability of isolated DNA bases: Adenine. *Proceedings of the National Academy of
640 Sciences* **2006**, *103*, 10196-10201.

641 [66] Ullrich, S.; Schultz, T.; Zgierski, M. Z.; Stolow, A., Electronic relaxation dynamics in DNA and RNA
642 bases studied by time-resolved photoelectron spectroscopy. *Physical Chemistry Chemical Physics* **2004**, *6*,
643 2796-2801.

644 [67] Buchner, F.; Heggen, B.; Ritze, H.-H.; Thiel, W.; Lübcke, A., Excited-state dynamics of guanosine in
645 aqueous solution revealed by time-resolved photoelectron spectroscopy: Experiment and theory. *Phys.
646 Chem. Chem. Phys.* **2015**, *17*, 31978-31987.

647 [68] Buchner, F.; Ritze, H. H.; Lahl, J.; Lübcke, A., Time-resolved Photoelectron Spectroscopy of Adenine
648 and Adenosine in Aqueous Solution. *Phys. Chem. Chem. Phys.* **2013**, *15*, 11402-11408.

649 [69] Cohen, B.; Hare, P. M.; Kohler, B., Ultrafast Excited-State Dynamics of Adenine and
650 Monomethylated Adenines in Solution: Implications for the Nonradiative Decay Mechanism. *Journal of
651 the American Chemical Society* **2003**, *125*, 13594-13601.

652 [70] Hare, P. M.; Crespo-Hernández, C. E.; Kohler, B., Internal conversion to the electronic ground state
653 occurs via two distinct pathways for pyrimidine bases in aqueous solution. *Proceedings of the National
654 Academy of Sciences* **2007**, *104*, 435-440.

655 [71] Pilles, B. M.; Maerz, B.; Chen, J.; Bucher, D. B.; Gilch, P.; Kohler, B.; Zinth, W.; Fingerhut, B. P.;
656 Schreier, W. J., Decay Pathways of Thymine Revisited. *The Journal of Physical Chemistry A* **2018**, *122*, 4819-
657 4828.

658 [72] Canuel, C.; Mons, M.; Piuzzi, F.; Tardivel, B.; Dimicoli, I.; Elhanine, M., Excited states dynamics of
659 DNA and RNA bases: Characterization of a stepwise deactivation pathway in the gas phase. *The Journal of
660 Chemical Physics* **2005**, *122*, 074316.

661 [73] Wolf, T. J. A.; Parrish, R. M.; Myhre, R. H.; Martínez, T. J.; Koch, H.; Gühr, M., Observation of
662 Ultrafast Intersystem Crossing in Thymine by Extreme Ultraviolet Time-Resolved Photoelectron
663 Spectroscopy. *The Journal of Physical Chemistry A* **2019**, *123*, 6897-6903.

664 [74] Improta, R.; Santoro, F.; Blancafort, L., Quantum Mechanical Studies on the Photophysics and the
665 Photochemistry of Nucleic Acids and Nucleobases. *Chemical Reviews* **2016**, *116*, 3540-3593.

666 [75] Liu, Y.; Chakraborty, P.; Matsika, S.; Weinacht, T., Excited state dynamics of *cis,cis*-1,3-
667 cyclooctadiene: UV pump VUV probe time-resolved photoelectron spectroscopy. *The Journal of Chemical
668 Physics* **2020**, *153*, 074301.

669 [76] Nugent-Glandorf, L.; Scheer, M.; Samuels, D. A.; Mulhisen, A. M.; Grant, E. R.; Yang, X. M.;
670 Bierbaum, V. M.; Leone, S. R., Ultrafast time-resolved soft x-ray photoelectron spectroscopy of dissociating
671 Br_2 . *Physical Review Letters* **2001**, *87*, 193002.

672 [77] Warne, E. M.; Downes-Ward, B.; Woodhouse, J.; Parkes, M. A.; Springate, E.; Pearcy, P. A. J.; Zhang, Y.;
673 Karras, G.; Wyatt, A. S.; Chapman, R. T.; Minns, R. S., Photodissociation dynamics of methyl iodide
674 probed using femtosecond extreme ultraviolet photoelectron spectroscopy. *Physical Chemistry Chemical
675 Physics* **2020**, *22*, 25695-25703.

676 [78] Brauße, F.; Goldsztejn, G.; Amini, K.; Boll, R.; Bari, S.; Bomme, C.; Brouard, M.; Burt, M.; de
677 Miranda, B. C.; Düsterer, S.; Erk, B.; Géléc, M.; Geneaux, R.; Gentleman, A. S.; Guillemin, R.; Ismail, I.;
678 Johnsson, P.; Journel, L.; Kierspel, T.; Köckert, H.; Küpper, J.; Lablanquie, P.; Lahli, J.; Lee, J. W. L.; Mackenzie,
679 S. R.; Maclot, S.; Manschwetus, B.; Mereshchenko, A. S.; Mullins, T.; Olshin, P. K.; Palaudoux, J.;
680 Patchkovskii, S.; Penent, F.; Piancastelli, M. N.; Rompotis, D.; Ruchon, T.; Rudenko, A.; Savelyev, E.; Schirmel,
681 N.; Techert, S.; Travnikova, O.; Trippel, S.; Underwood, J. G.; Vallance, C.; Wiese, J.; Simon, M.; Holland, D.
682 M. P.; Marchenko, T.; Rouzée, A.; Rolles, D., Time-resolved inner-shell photoelectron spectroscopy: From a
683 bound molecule to an isolated atom. *Physical Review A* **2018**, *97*, 043429.

684 [79] Mayer, D.; Lever, F.; Picconi, D.; Metje, J.; Alisauskas, S.; Calegari, F.; Düsterer, S.; Ehlert, C.; Feifel,
685 R.; Niebuhr, M.; Manschwetus, B.; Kuhlmann, M.; Mazza, T.; Robinson, M. S.; Squibb, R. J.; Trabattoni, A.;
686 Wallner, M.; Saalfrank, P.; Wolf, T. J. A.; Gühr, M., Following excited-state chemical shifts in molecular
687 ultrafast x-ray photoelectron spectroscopy. *Nature Communications* **2022**, *13*, 198.

688 [80] Corkum, P. B., Plasma perspective on strong field multiphoton ionization. *Physical Review Letters*
689 **1993**, *71*, 1994-1997.

690 [81] Schuurman, M. S.; Blanchet, V., Time-resolved photoelectron spectroscopy: the continuing
691 evolution of a mature technique. *Physical Chemistry Chemical Physics* **2022**, *24*, 20012-20024.

692 [82] Poletto, L.; Frassetto, F., Time-preserving grating monochromators for ultrafast extreme-ultraviolet
693 pulses. *Applied Optics* **2010**, *49*, 5465-5473.

694 [83] Ojeda, J.; Arrell, C. A.; Longetti, L.; Chergui, M.; Helbing, J., Charge-transfer and Impulsive
695 Electronic-to-vibrational Energy Conversion in Ferricyanide: Ultrafast Photoelectron and Transient Infrared
696 Studies. *Phys. Chem. Chem. Phys.* **2017**, *19*, 17052-17062.

697 [84] Ban, L.; Yoder, B. L.; Signorell, R., Size-Resolved Electron Solvation in Neutral Water Clusters. *The
698 Journal of Physical Chemistry A* **2021**, *125*, 5326-5334.

699 [85] Ojeda, J.; Arrell, C. A.; Grilj, J.; Frassetto, F.; Mewes, L.; Zhang, H.; Mourik, F. v.; Poletto, L.; Chergui,
700 M., Harmonium: A pulse preserving source of monochromatic extreme ultraviolet (30–110 eV) radiation
701 for ultrafast photoelectron spectroscopy of liquids. *Structural Dynamics* **2016**, *3*, 023602.

702 [86] Thurmer, S.; Malerz, S.; Trinter, F.; Hergenhahn, U.; Lee, C.; Neumark, D. M.; Meijer, G.; Winter, B.;
703 Wilkinson, I., Accurate vertical ionization energy and work function determinations of liquid water and
704 aqueous solutions. *Chemical Science* **2021**, *12*, 10558-10582.

705 [87] West, C. W.; Nishitani, J.; Higashimura, C.; Suzuki, T., Extreme ultraviolet time-resolved
706 photoelectron spectroscopy of aqueous aniline solution: enhanced surface concentration and pump-
707 induced space charge effect. *Molecular Physics* **2021**, *119*, e1748240.

708 [88] Longetti, L.; Barillot, T. R.; Puppin, M.; Ojeda, J.; Poletto, L.; van Mourik, F.; Arrell, C. A.; Chergui,
709 M., Ultrafast photoelectron spectroscopy of photoexcited aqueous ferrioxalate. *Physical Chemistry
710 Chemical Physics* **2021**, *23*, 25308-25316.

711 [89] Sutherland, J. R.; Christensen, E. L.; Powers, N. D.; Rhynard, S. E.; Painter, J. C.; Peatross, J., High
712 harmonic generation in a semi-infinite gas cell. *Opt. Express* **2004**, *12*, 4430-4436.

713 [90] Falcão-Filho, E. L.; Gkortsas, V. M.; Gordon, A.; Kärtner, F. X., Analytic scaling analysis of high
714 harmonic generation conversion efficiency. *Opt. Express* **2009**, *17*, 11217-11229.

715

716